

Experimental study on seismic performance of concrete filled tubular square column-to-beam connections with combined cross diaphragm

Sung-Mo Choi[†]

School of Architecture and Architectural Engineering, University of Seoul, Seoul, 130-743, Korea

Yeo-Sang Yun[‡]

Harmony Structural Engineering, Seoul, Korea

Jin-Ho Kim[‡]

*Research Institute of Industrial Science & Technology Steel Structure Research Laboratory,
Kyungkido, 445-813, Korea*

(Received April 20, 2005, Accepted February 14, 2006)

Abstract. The connection with combined cross diaphragm is developed for the connection of square CFT column and steel beam and proposed to be used for the frame with asymmetric span length. The structural characteristics of this connection lie in the penetration of the beam flange in the direction of major axis through the column for the smooth flow of stress. The purpose of this study is to analyze the dynamic behavior and stress flow of suggested connection and to evaluate the resistance to shock of connection. Four T-type CFT column-to-beam specimens; two with combined cross diaphragm and the others with interior and through diaphragms, the existing connection types, were made for cyclic load test guided by the load program of ANSI/AISC SSPEC 2002. The results show that the proposed connection is more efficient than existing ones in terms of strength, stress flow and energy absorption and satisfies the seismic performance required in the region of weak/moderate earthquakes.

Keywords: concrete filled tube (CFT); combined cross diaphragm; column-to-beam connection; cyclic loading program.

1. Introduction

Regarded as the structure of high ductility, the steel moment resisting frame is widely used as structural system for high-rise buildings. Square CFT column has been recently drawing attention, to be utilized in these steel moment frames (Alostaz and Schneider 1996, Schneider and Alostaz 1998, Kato 1992, Han 2000, Mohammad 1997, Choi 2002). Featuring closed cross-section, it is characterized by

[†]Professor, Corresponding author, E-mail: smc@uos.ac.kr

[‡]Research Associate

efficiency due to the composition of steel tube resisting flexure outside and concrete resisting axial force inside. It presents excellent deformation ability attributable to constraint of local buckling of steel tube by filled concrete (Hiroyuki 1998). Such structural characteristics of square CFT structure make it suitable for the structure of high-rise buildings (Cheng and Chung 2003, Chou and Uang 2002, Chi and Uang 2002, Storozhenko *et al.* 1998, Wang 1997). However, disadvantage associated with closed cross-section and complicity of column-to-beam connection reinforcement such as inserting diaphragm for restraining out-of-plane deformation of column set limits to its field application, in spite of its material excellence as structure member. Thus, many studies have been conducted worldwide to solve these problems of CFT column-to-beam connection.

Researches related to connection reinforcement with diaphragm have been active in Japan where square steel tubes are commonly used as column member of steel structures. Through and interior diaphragms have been most commonly used for reinforcement of connection. Connections with interior diaphragms involve excessive tensile stress at steel tube face in contact with the beam flange, since beam flange of long span is relatively thicker than column flange. Then, tensile stress results in lamellar tearing, which may cause early brittle fracture at connection. Connections with through diaphragm have the merit of smooth transfer of stress, since diaphragm penetrates steel tube to be directly welded into beam flange. But, construction work is complicated and field welding is required. When beam flange is thick, welding consequently increases due to the increase of diaphragm thickness, which accompanies the burden of welding quality management and inspection. In addition, it contains the possibility of brittle fracture at weld zone of connection attributable to stress concentration caused by sudden form change in the contact of beam flange and diaphragm. The earthquakes in Northridge, U.S.A. and Gobe, Japan were the case presenting shortcomings in seismic performance of connections of steel moment frames. They also showed that even steel structure could not present ductile behavior unless ductility was secured by the appropriate details of connection (SAC Joint Venture 2000a).

This study suggests a new type of connection with combined cross diaphragm, as shown in Fig. 1, which can reduce out-of-plane deformation of flange of steel tube column and enhance serviceability, as an alternative to the existing connection types. Combined cross diaphragm features detail improvement for smooth delivery of stress and mitigation of stress concentration. Also, it was designed to be suited

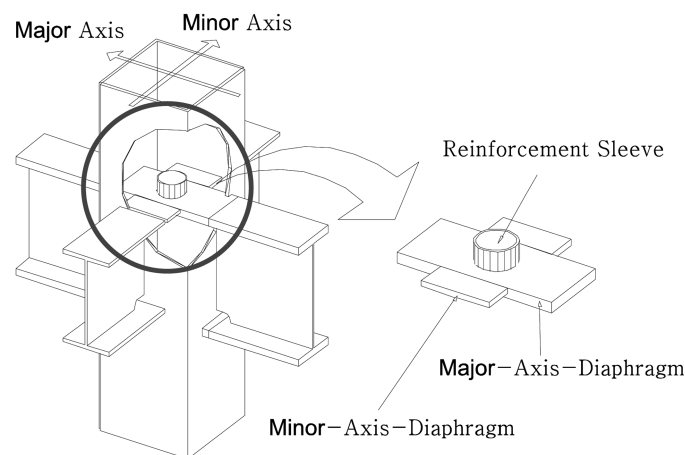


Fig. 1 Combined cross diaphragm

for load transfer mechanism by short/long span ratio. As for the tensile side of column-to-beam connection to which relatively major flexure is applied (major axis), major axis diaphragm of the same width as that of beam flange penetrated steel tube flange to be directly connected to beam flange. This can reduce stress concentration caused by sudden shape change which is the problem associated with the connection with through diaphragm. As for tensile side to which relatively minor flexure is applied (minor axis), minor axis diaphragm was inserted inside column as in connections with interior diaphragm; but the difference lies in the width of diaphragm same as that of beam flange. This provides diaphragm and column flange with sufficient deformation ability, resulting in reduced stress concentration. For concrete filling, opening ratio was ensured by a circular opening made at the center of diaphragm, if the opening area obtained from subtraction of area of diaphragm from area of column was less than 15%. To have filled-concrete compensate for the loss of cross-sectional area, a cylinder-shaped sleeve was welded into diaphragm to play a role of an anchor. The sleeve was designed with commercially used structural steel pipe. It was 6 mm thick and protruded with the length of as much as its diameter from the diaphragm up and down each.

Authors examined structural behavior of the diaphragm as a member of connection through experiment and analysis on the simple tension behavior of combined cross diaphragm in the previous study (Choi 2003, 2004, 2005, Cha 2002, Hong 2002, 2004, Yun 2002, 2002, 2005). The purpose of this study is to develop a new connection type which is superior to the existing types in terms of construction work and structural performance and suitable for the structures in the regions of weak/moderate earthquakes. So, based on the previous study, T-shaped column-to-beam connection specimens were made in actual size and cyclic load tests on these specimens were performed using load program of ANSI/AISC SSPEC-2002 (AISC Seismic Provisions No.2, Part I 2002). Then, parameter study was conducted to examine the behavior of connections.

2. Test plan

2.1. Specimens plan

In all specimens, columns were square tubular section of \square -400×400×12 made of SM490 rolled steel as stipulated in Korean Industrial Standards to be used for welded structures, and beams were wide flange section of H-500×200×10×16, SS400 rolled steel as required by Korean Industrial Standards to be used for general structures. The steel tubular column was filled with high-flexible concrete of 28-day compressive strength, 49 MPa.

Figs. 2, 3, 4 and 5 show the details of each specimen and Table 1 summarizes the characteristics of specimens. Specimen ID (interior diaphragm) adopts existing connection type with 16 mm thick interior diaphragm. Diameter of opening in diaphragm is 227 mm and air vent hole of 25 mm in diameter was used to enhance concrete filling. Opening ratio is 30%, to comply with construction regulations. Specimen TD adopts the existing connection type with through diaphragm of 16 mm in thickness and 460 mm in length. Diameter of opening in diaphragm is 227 mm and diameter of air vent hole is 25 mm. Opening ratio is 30%, same as that of specimen ID. The diaphragm is exposed outside the column flange with the length of 30 mm. Specimen CDS adopts connections with combined cross diaphragm reinforced with sleeve. Both major and minor axis diaphragms are 200 mm wide and 16-mm thick. Cylinder-shaped sleeve is inserted at the center of diaphragm, which is 6 mm thick, 130 mm long and 114.3 mm in diameter. Actual opening ratio is 28.4% due to the sleeve inserted in diaphragm. Specimen CD

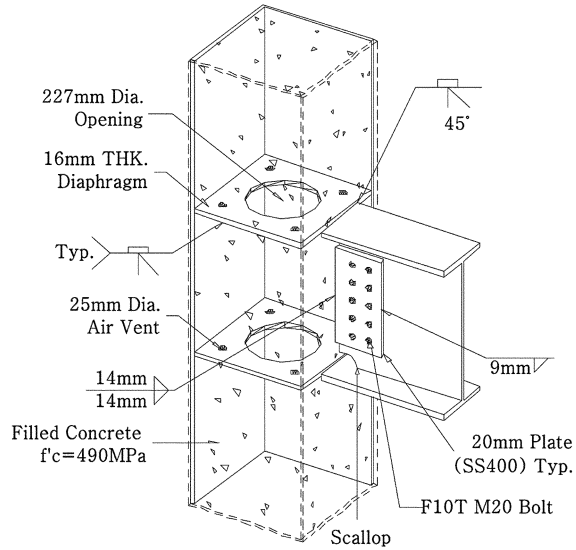


Fig. 2 Interior diaphragm (ID) details

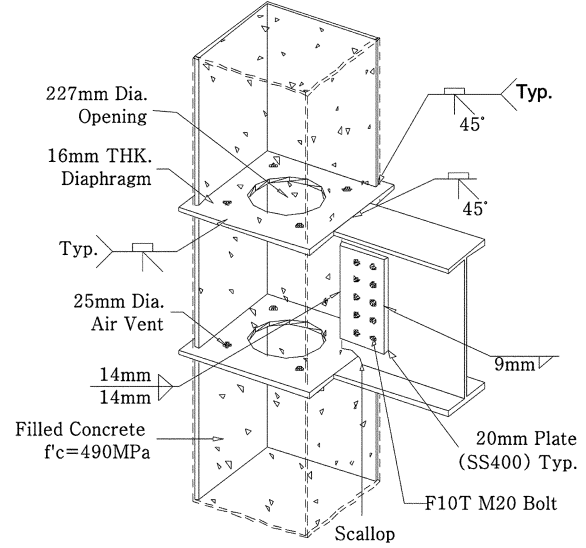


Fig. 3 Through diaphragm (TD) details

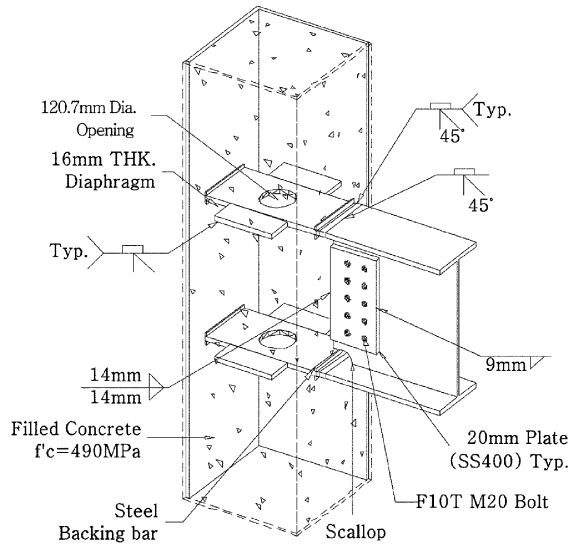


Fig. 4 Combined cross diaphragm (CD) details

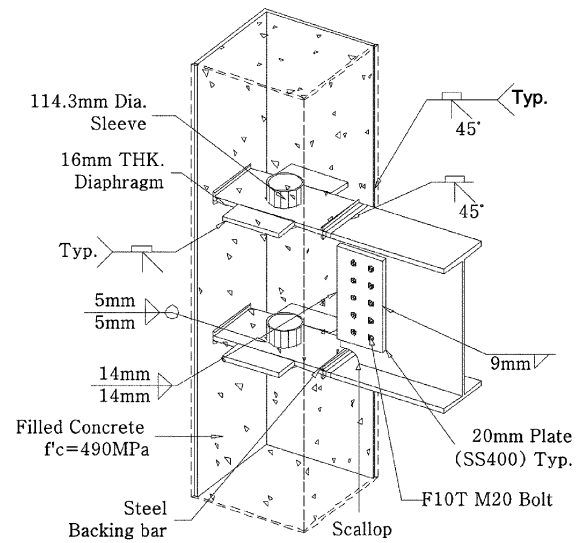


Fig. 5 Combined cross diaphragm (CDS) details (with sleeve reinforcement)

adopts connections with combined cross diaphragm which is not reinforced with sleeve. Diameter of opening in diaphragm is 120.7 mm and the other details of specimen CD are same as those of specimen CDS except that there isn't sleeve in diaphragm of specimen CD.

Sleeve was inserted to compensate the reduced tensile strength of diaphragm caused by the loss in the cross-sectional area due to the opening in diaphragm, that is, to ensure the resistance against in-plane stress generated on diaphragm by the transfer of tension from beam flange. In the previous study, authors suggested the capacity evaluation equations of the connection including the sleeve through the

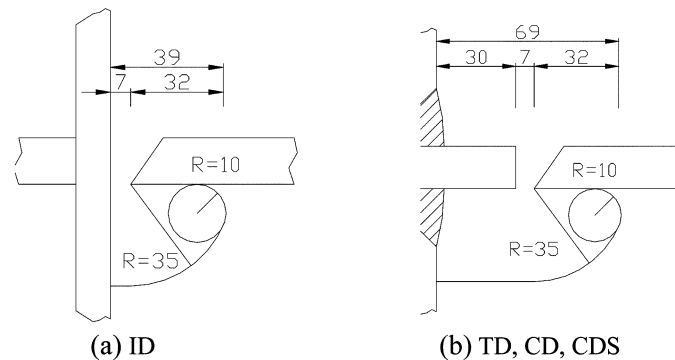


Fig. 6 Scallop details

Table 1 Specimen description

Specimen	Diaphragm type	With/Without Sleeve [†]	Diaphragm size
ID	Interior	-	PL 376 mm×376 mm ($t=16$ mm) with Φ 227 mm opening
TD	Through	-	PL 460 mm×460 mm ($t=16$ mm) with Φ 227 mm opening
CD	Combined cross	-	Major-axis: Φ 120.7 mm opening, $b=200$ mm, $t=16$ mm
CDS	Combined cross	O	Minor-axis: $b=200$ mm, $t=16$ mm

[†] Φ 114.3×6 mm, $L=130$ mm

Table 2 Mechanical properties

Element	THK. (mm)	σ_y (MPa)	σ_u (MPa)	E (MPa)
Column	12	472	616	2.1
Beam web	10	347	460	2.1
Beam flange	16	349	488	1.9
Concrete		$f'_c = 49$ MPa		

experiment on the stress transfer through the sleeve which is one of the important components of the CFT column-to-beam connection with combined cross diaphragm (Choi 2005).

Welding was done by FCAM method (Flux-Cored Arc Welding) using E71T-1 ϕ 1.6 mm electrode stick. Commonly adopted for shop welding in Korea, this welding method complies with AWS (American Welding Society) standards. SMAW (Shielded Metal Arc Welding) method using E7018 ϕ 1.8 mm electrode stick was used for welding between steel tube and beam flange. The end of one member to weld was cut diagonally for better welding condition and welded to the other by groove welds, as shown in Fig. 6. When it was difficult to weld inside steel tube, backing bars were used for welding of steel tube and steel tube, steel tube and diaphragm and beam flange and diaphragm, in order to prevent weld defects such as shrinkage and crack and slag inflow which could possibly occur at the beginning of welding and affect test results. Steel tube and beam flange were connected by full penetration welding and scallop of 35 mm in diameter was placed at both edges of beam web, to be identical to the field welding.

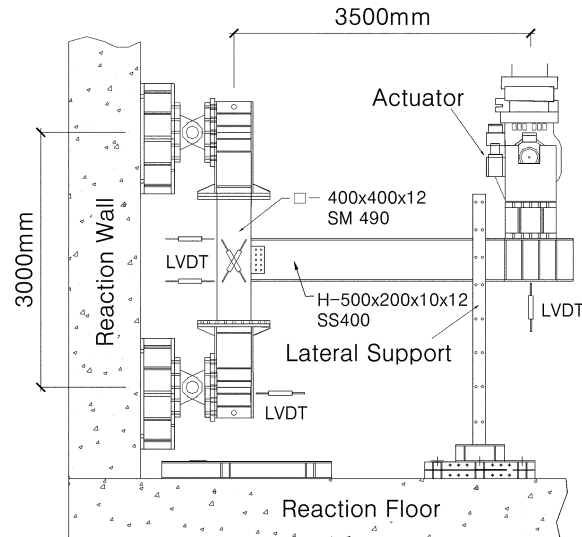


Fig. 7 Test set-up

2.2. Material test

To examine the mechanical properties of steel material used for specimens, tensile strength test was carried out on 3 pieces from each material guided by the provisions of KS B 0802, Method of Tensile Test for Metallic Material in Korean Standard. The materials used in tensile strength test were 12 mm thick plate of SM490 steel and 10 mm and 16 mm thick plates of SS400 steel. 28-day compression test was conducted on concrete. Table 2 presents the material test results; the thickness, modulus of elasticity (E), yield strength (σ_y) and tensile strength (σ_u) of steel and 28-day compressive strength (f'_c) of concrete, which are the averages of test data for each material.

2.3. Test setup

Specimens were set up using reaction wall and floor as shown in Fig. 7. To model the frame with horizontal load applied to column-to-beam connections, top and bottom ends of column were hinged at reaction wall parallel to column and an actuator with the capacity of 1960 KN was mounted on the end of beam for cyclic load application in vertical direction. In addition, supplementary supports were installed at both edges of load application point to prevent lateral-torsional buckling of beam.

2.4. Loading history

Displacement-controlled load was applied by ANSI/AISC SSPEC-2002 Cyclic Loading Program (AISC Seismic Provisions No.2, Part I 2002) as shown in Fig. 8. Displacement at the edge of beam was decided by drift angle using the distance between load application point and column center (Giton and Uang 2002, AISC Seismic Provisions No.2, Part II 2000). 6 cycles of load was applied at the drift angles of 0.375, 0.5 and 0.75%, 1 cycle at 1%, and 2 cycles after 2%. 2 cycles of load was applied at every 1% increase, after drift angle of 3% up to failure.

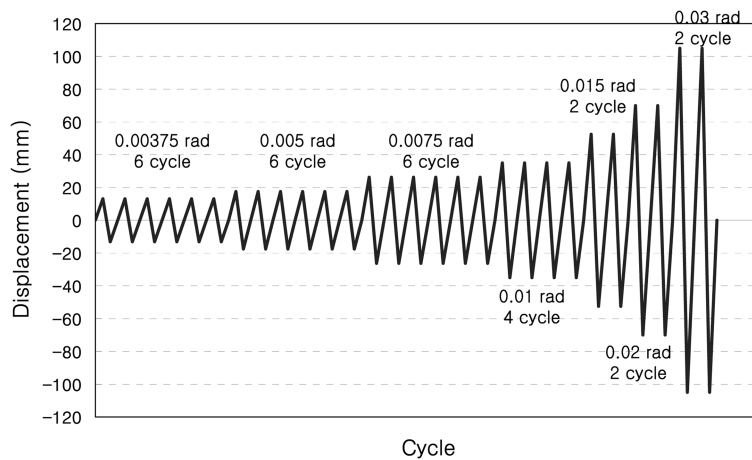


Fig. 8 ANSI/AISC SSPEC-2002

2.5. Measurement instrumentation

Strain gages and linear variable displacement transducers were installed for the examination of overall behavior and local deformation. Specimen displacement was controlled by vertical displacement of actuator. The magnitude of applied load was measured by load cell of actuator. Guided by Seismic Provisions for Structural Steel Building, inelastic rotation angle for the evaluation of ductility (AISC Seismic Provisions No.2, Part II 2000) was calculated by estimating inelastic behavior at the intersection of centerlines of column and beam.

3. Test results and analysis

3.1. Relation between moment and rotation angle

3.1.1. Specimen ID (Interior Diaphragm)

Specimen ID adopting the existing connections with interior diaphragm remained elastic up to third step (0.0075 rad.), prior to undergoing elastic-plastic behavior. At third step, the surface of beam flange started falling off, showing the sign of yield. During fourth step (0.01 rad.), the surface of beam flange fell off extensively and plasticization began, but crack was not yet observed. Micro-cracking started between upper steel tube and beam flange at fifth step (0.015 rad.), and cracking continued during sixth step accompanied with reduced strength. Ultimate strength was reached at seventh step (0.03 rad.) followed by failure due to tearing of steel tube and beam flange, as shown in Fig. 9(b). Ultimate strength exceeded plastic moment of beam (M_p ; dotted line), as shown in Fig. 9(a).

3.1.2. Specimen TD (Through Diaphragm)

The hysteretic curve of specimen TD is shown in Fig. 10(a). Specimen TD presented elastic behavior up to third step (0.0075 rad.) and elasto-plastic behavior accompanied with the sign of yield afterwards. At fifth step (0.015 rad.), yielding and cracking at the welding of lower beam flange and diaphragm started. Then, cracking in the weld zone of lower and upper beam flanges was increased

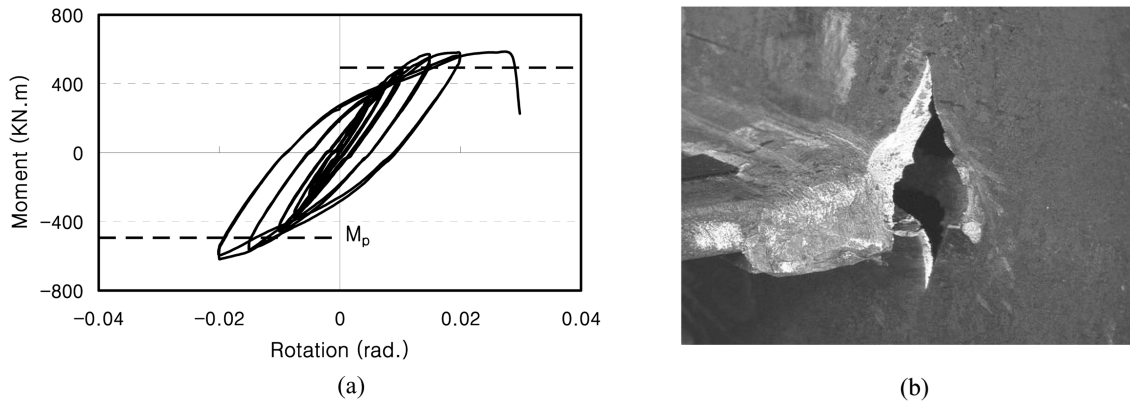


Fig. 9 Answer curves of specimen ID (a) moment-rotation angle (b) final failure (0.03 rad.)

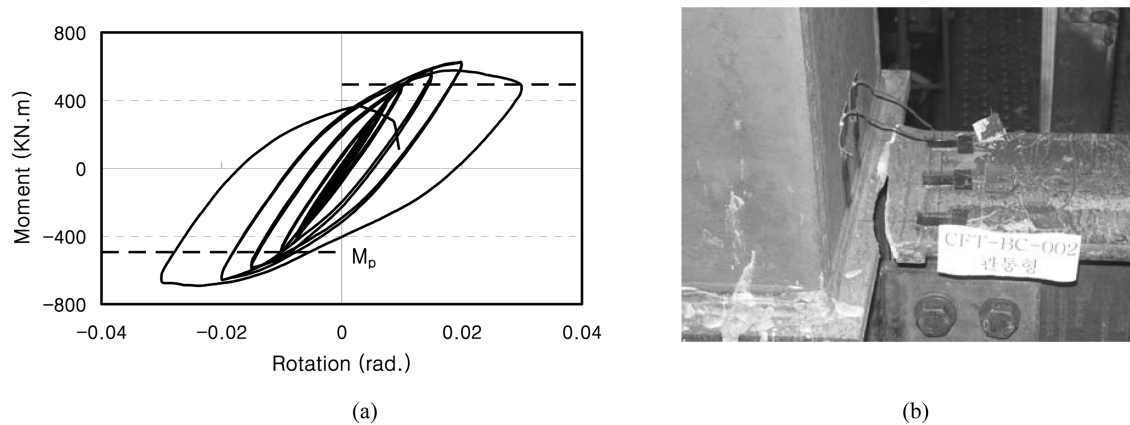


Fig. 10 Answer curves of specimen TD (a) moment-rotation angle (b) final failure (0.03 rad.)

due to stress concentration on edges caused by repeated load application. At sixth step (0.02 rad.), sudden decrease of strength was observed. Test ended with the failure of weld zone between upper beam flange and diaphragm as shown in Fig. 10(b), after ultimate strength was reached at seventh step.

3.1.3. Specimen CD (Combined Cross Diaphragm without Reinforcement)

Specimen CD showed stable hysteretic curves up to third step (0.07 rad.) as shown in Fig. 11(a). After third step, it showed plastic behavior along with yielding of beam flange, though no external change was observed. At fifth step (0.015 rad.), yielding started at lower steel tube and micro cracking was observed at the welding of the diaphragm outside steel tube and steel tube. It is inferred that this is because diaphragm yielded before yielding of beam flange, due to the loss in cross-sectional area of major axis diaphragm. Sixth step presented apparent crack at weld zone between diaphragm and steel tube, but no other fine crack was observed. At seventh step, welding zone between flanges of steel tube started to crack accompanying abrupt decrease of stiffness. Test ended with fracture at welding between steel tube flanges as shown in Fig. 11(b), after ultimate strength was reached at seventh step.

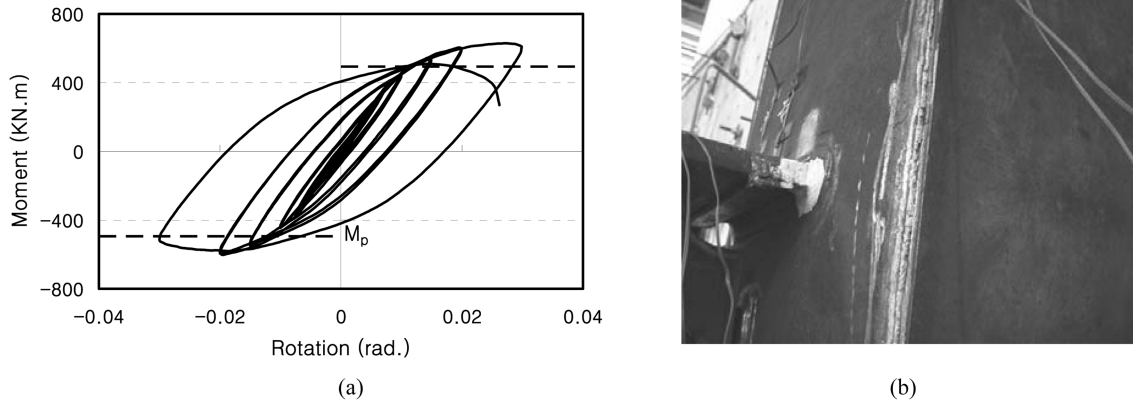


Fig. 11 Answer curves of specimen CD (a) moment-rotation angle (b) final failure (0.03 rad.)

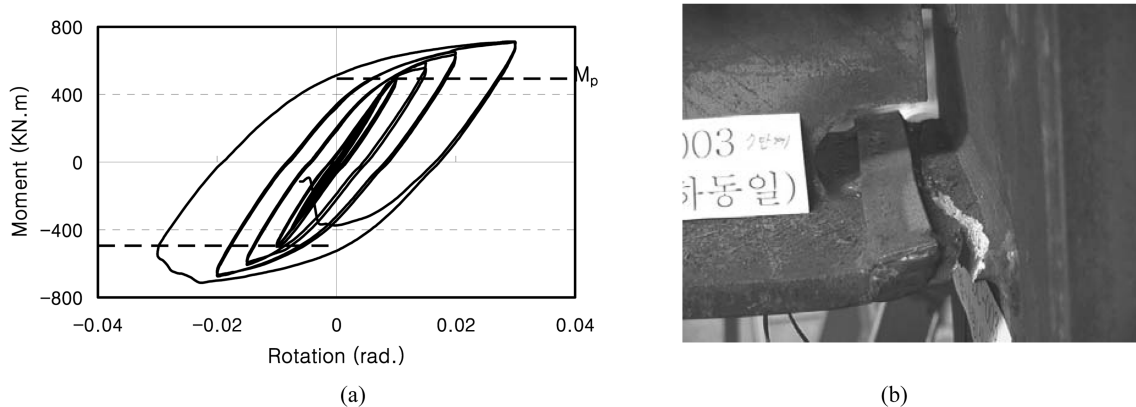


Fig. 12 Answer curves of specimen CDS (a) moment-rotation angle (b) final failure (0.03 rad.)

3.1.4 Specimen CDS (Combined Cross Diaphragm with Sleeve Reinforcement)

Specimen CDS presented very stable hysteretic curves as shown in Fig. 12(a). Though the surface of beam flange fell off at third step (0.00375 rad.), it showed still elastic behavior. No external change was observed until fifth step. At sixth step (0.02 rad.), tension cracking started due to necking of exterior diaphragm following the yielding of beam flange, and cracking propagated with decrease in strength, during sixth and seventh step (0.03 rad.). After ultimate strength was reached at seventh cycle (0.03 rad.), test ended with the failure of diaphragm as shown in Fig. 12(b), which is due to the hardening of exterior diaphragm caused by the welding of diaphragm with steel tube and beam flange. The strength exceeded plastic moment of beam as shown in Fig. 12(a).

3.2. Initial stiffness and ultimate strength

Fig. 13 shows monotonic graphs to which hysteretic curves for moment-rotation angle of specimens are converted. Deviation shown at the center of the curves is attributable to slippage of hinge at top and bottom of the column. When the upper beam flange was in tension, the specimen CDS with sleeve

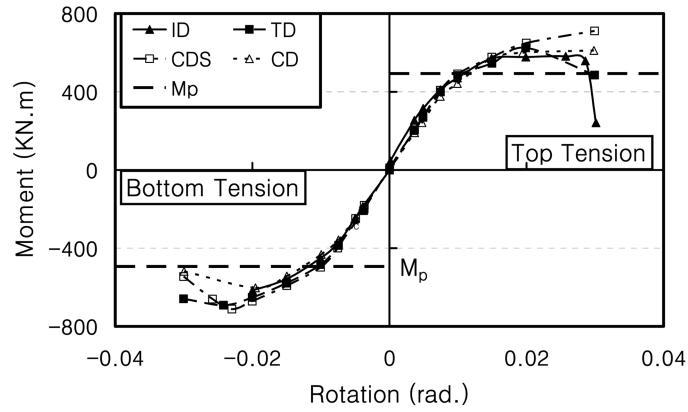


Fig. 13 Monotonic curves of moment-rotation angle relation

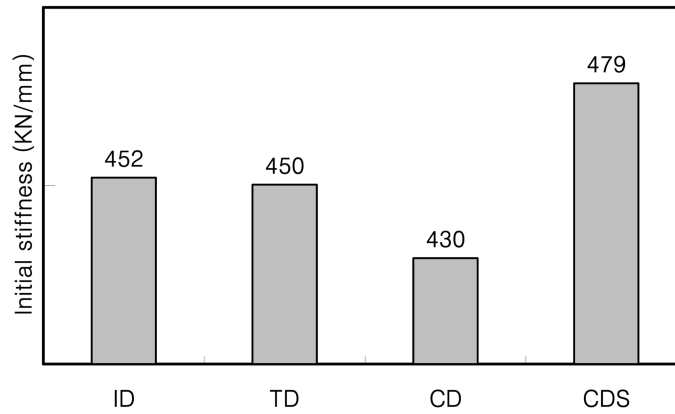


Fig. 14 Initial stiffness of specimens

reinforcement presented the highest strength and very stable hysteretic curve. On the contrary, the specimen CD without sleeve reinforcement presented strength similar to those of specimens ID and TD, but its hysteretic curve was stable without rapid decrease of strength, ascribable to smooth delivery of stress.

Under the condition that upper flange was in compression, the specimens CDS and TD and the specimens CD and ID yielded similar values in ultimate strength, respectively. Specimen CDS featured similar strength to that under upper tension, but rapid decrease of strength was observed after the point where ultimate strength was decided. The specimen CD presented relatively lower strength compared with CDS, in both cases of upper tension and upper compression, which is inferred to be ascribable to the absence of sleeve reinforcement of diaphragm.

Fig. 14 shows initial stiffness of each specimen. Among the similar values of strength associated with each specimen, initial stiffness of CDS is slightly higher than those of the others. Initial stiffness of the specimen CD is relatively lower than those of ID and TD. As shown in Fig. 13, the stiffness of every specimen was getting lower as it entered plasticity after passing through elastic range. While the specimen CDS presented stable behavior with gradual decrease of stiffness, other specimens accompanied rapid

decrease of stiffness after entering plastic status. It is inferred that smooth flow of stress between beam flange and diaphragm of specimen CDS prevented stiffness from decreasing suddenly.

3.3. Strain distribution by load-step

Comparison of strain distribution was made between the existing diaphragms and combined cross diaphragm with the values measured by strain gauge installed in beam flange of each specimen. Fig. 15 shows strain distribution of beam flange by load-step at 0.015 rad with upper flange in tension.

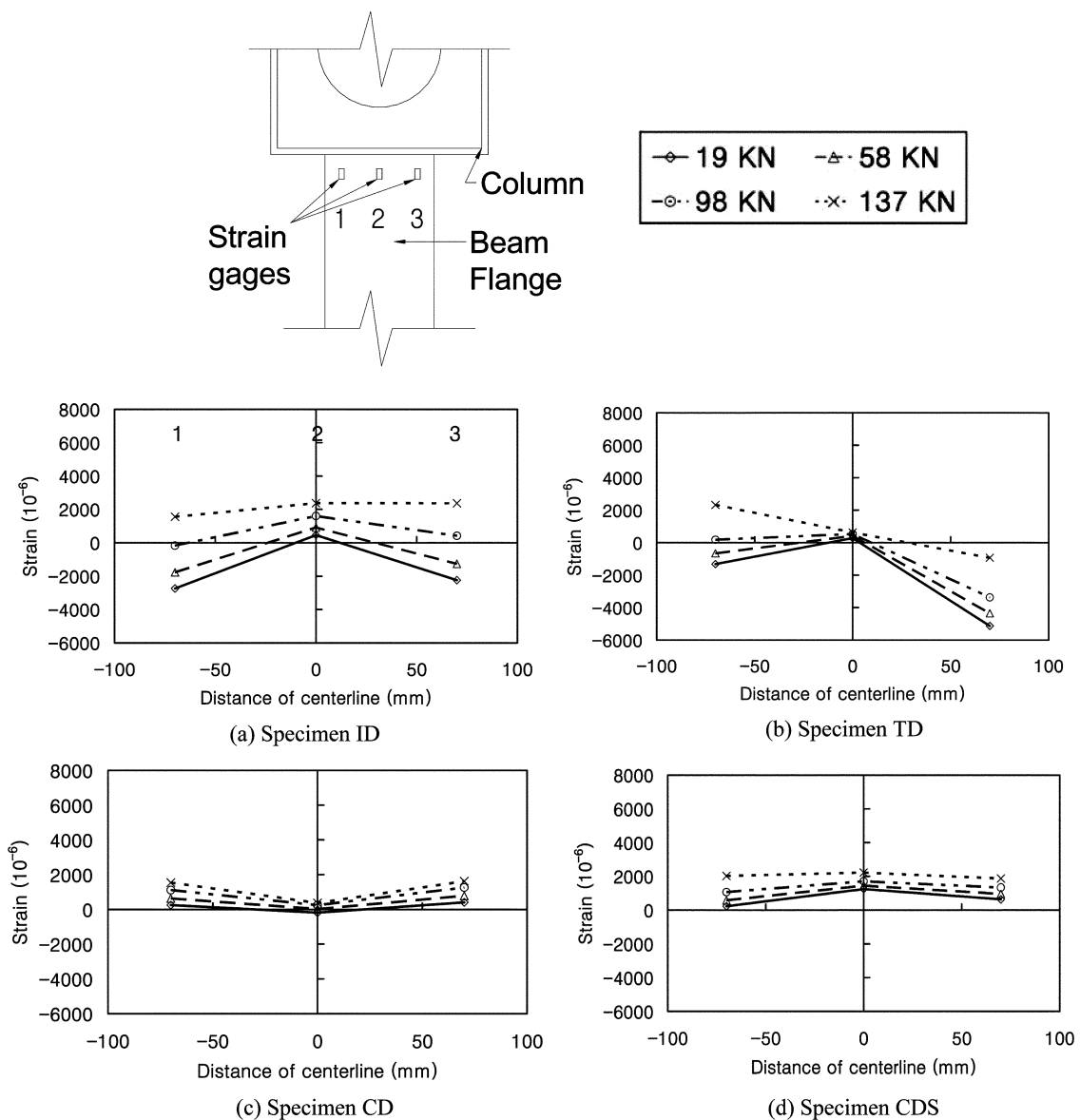


Fig. 15 Strain distribution of beam flange by load-step (Cheng and Chung 2003)

0.015 rad was chosen to examine stress flow of beam flange under plastic status after yielding, since every specimen yielded at 0.015 rad.

The specimens ID and TD presented larger strain in both edges than in the center of beam as load increased. It is inferred that abrupt geometric form change of diaphragm in connections of beam flange and diaphragm made stress concentrate on both edges. The specimens CDS and CD showed uniform distribution of strain throughout whole cross-sectional area of beam. It seems that stress concentration was reduced since tensile force of beam flange was delivered to diaphragm of the same width as that of beam flange.

3.4. Plastic rotation capacity

The plastic deformation capacity to absorb large energy is essential to the column-to-beam connection of the structure under the earthquake. Table 3 shows plastic rotation capacity requirements suggested by AISC, Seismic Provisions for Structural Steel Buildings by frame and Fig. 16 shows moment-inelastic rotation angle curve of each specimen after seventh step ($\delta = 105$ mm). All specimens reached 0.02 rad of rotation angle. However, the specimen ID and TD presented somewhat unstable curves while specimen with combined cross diaphragm showed stable hysteretic curves even after 0.02 rad. According to the seismic regulations by AISC, the CDS specimen can be classified as composite intermediate moment frame, which can be used in the regions of moderate earthquakes. Accordingly, it can be said that the connection adopted in the specimen CDS is applicable for the structures in the regions of weak/moderate earthquakes such as Korea.

Table 3 Seismic performance requirement by frame (AISC Seismic Provisions No.2, Part II 2000)

Frame classifications	Connection plastic rotation capacity (rad)
OMF : Ordinary Moment Frame	0.01
IMF : Intermediate Moment Frame	0.02
SMF : Special Moment Frame	0.03

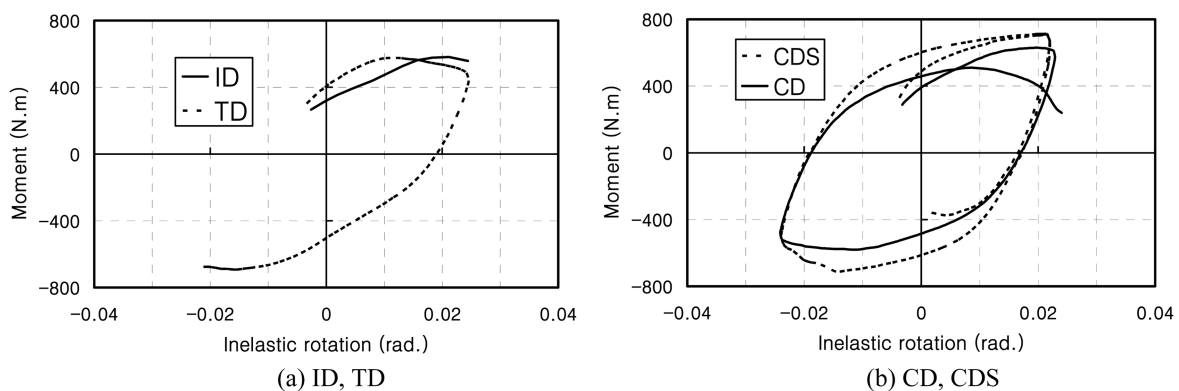


Fig. 16 Moment-inelastic rotation angle curves after 7th step ($\delta = 105$ mm)

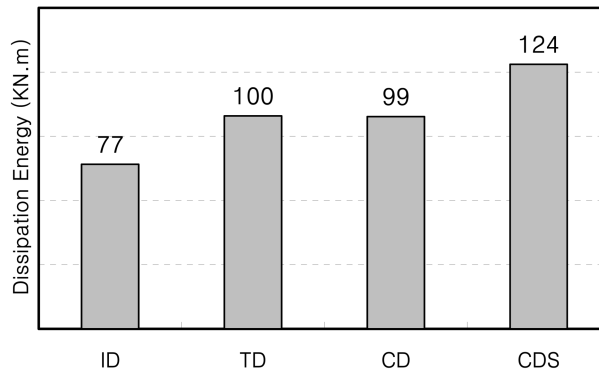


Fig. 17 comparison of energy dissipation

3.5. Energy absorption capacity

The dissipation of energy is one of important seismic performances of structure. Dissipated energy can be measured by the accumulation of the area enclosed by load-displacement hysteretic graphs and also evaluated by total plastic work done by the structure. Fig. 17 shows the comparison of energy absorbed by beam of each specimen until failure. From the comparison between specimens CDS and CD, it is observed that inserting sleeve in diaphragm increases energy absorbing capacity of connection. It is because the absence of sleeve lowers composite effect between diaphragm and concrete and thus reduces strength. The comparison between specimen ID and others shows that direct connection of diaphragm and beam flange increases energy dissipation more than connection of steel tube and beam flange. Energy dissipation of specimen CDS was the largest. We think the reason as follows: The sleeve inside of the steel tube increased the restraint of concrete and diaphragm. Also, the stress concentration at the joint of the interior diaphragm and concrete decreased and compression failure of concrete filled the steel tube was reduced. As a result, CDS specimen had the largest energy dissipation.

4. Conclusions

This study suggested new details for CFT column-to-beam connections reinforced with combined cross diaphragm. Test results showed that the connection with combined cross diaphragm reduced stress concentration and presented smooth flow of stress with uniform distribution of strain throughout beam flange. In addition, combined cross diaphragm increased ultimate strength and initial stiffness of connection. Especially, sleeve reinforcement of combined cross diaphragm contributed to the increase in initial stiffness and energy absorbing capacity. Featuring inelastic rotation angle of 0.02 rad, connection with combined cross diaphragm presented better deformation capacity than the existing connection types.

The failures of specimens at the welding zone show that the stable ductile behavior of connection requires the minimization of excessive stress at heat-affected parts caused by welding heat applied to column-to-beam connection, shear of beam flange and notch at welded parts.

Acknowledgments

This study was sponsored by the year 2002 support for construction research program of Samsung Heavy Industries Co., Ltd. and supported by Research Institute of Industrial Science & Technology. We like to express our heartfelt thanks to them for their support.

References

- Alostaz, Y. M. and Schneider, S. P. (1996), "Analytical behavior of connections to concrete-filled steel tubes", *J. Construct. Steel Res.*, **40**(2), 95-127.
- American Institute of Steel Construction, Inc (2000), Seismic Provisions for Structural Steel Buildings. Supplement No. 2, Part II, Chapter 9.
- American Institute of Steel Construction, Inc (2002), Seismic Provisions for Structural Steel Buildings. Supplement No. 2, Part I, Appendix S.
- Beutel, J., Thambiratnam, D. and Perera, N. (2001), "Monotonic behavior of composite column to beam connections", *Eng. Struct.*, **23**, 1152-1161.
- Beutel, J., Thambiratnam, D. and Perera, N. (2002), "Cyclic behavior of concrete filled steel tubular column to steel beam connections", *Eng. Struct.*, **24**(1), 29-38.
- Cha, E. J., Kim, Y. S., Kim, J. H. and Choi, S. M. (2002), "Reliability analysis for CFT column-to-beam connections with new diaphragm", *Proc. of Int. Symp. on Steel Structures: The Second, Korean Society of Steel Structures*, 103-114.
- Cheng, C. T. and Chung, L. L. (2003), "Seismic performance of steel beams to concrete-filled steel tubular column connections", *J. Construct. Steel Res.*, **59**(3), 405-426.
- Chi, B. and Uang, C. M. (2002), "Cyclic response and design recommendations of reduced beam section moment connections with deep columns", *J. Struct. Eng.*, ASCE, **128**(4), 464-473.
- Choi, S. M. and Kim, D. K. (2002), "CFT Standard (2000 Edition) and Development on CFT Connections in Korea", *7th Int. Conf. on Steel & Space Structures*: 2-3 October, Singapore, 9-18.
- Choi, S. M., Hong, S. D., Kim, D. K., Kim, Y. S. and Kim, J. H. (2004), "Structural capacities of tension side for CFT square column-to-beam connections with combined-cross-diaphragm", *Pacific Structural Steel Conference*.
- Choi, S. M., Hong, S. D., Kim, Y. S. and Kim, J. H. (2004), "Structural performance of tension side for CFT square column-to-beam connections with combined cross diaphragm", Architectural Institute of Korea, 23-32.
- Choi, S. M., Jung, D. S., Kim, D. J., Kim, J. H. (2005), "A study on the equations for load carrying capacities of concrete filled tubular square column-to-beam connections with combined cross diaphragm and sleeves", Korean Society of Steel Construction, 419-429.
- Choi, S. M., Yun, Y. S., Kim, D. K., Kim, Y. S. and Kim, J. H. (2004), "An experimental study on seismic performance of concrete filled tubular square column-to-beam connections with combined cross diaphragm", *Pacific Structural Steel Conference*.
- Choi, S. M., Yun, Y. S., Kim, Y. S. and Kim, J. H. (2003), "A study on seismic performance for CFT square column-to-beam connections reinforced with asymmetric lower diaphragms", Korean Society of Steel Construction, 579-589.
- Choi, S. M., Yun, Y. S., Kim, Y. S. and Kim, J. H. (2004), "An experimental study on seismic performance of concrete filled tubular square column-to-beam connections with combined cross diaphragm", Architectural Institute of Korea, 33-40.
- Chou, C. C. and Uang, C. M. (2002), "Cyclic performance of a type of steel beam to steel-encased reinforced concrete column moment connections", *J. Construct. Steel Res.*, **58**(5-8), 637-663.
- Han, L. (2000), "Influence of concrete compaction on the strength of concrete filled steel tubes", *Advance Structure Engineering*, **32**, 131-137.
- Hiroiyuki, N. (1998), "Analytical model for compressive behavior of concrete filled square steel tubular columns", *Trans. Jpn. Concr. Inst.* **20**, 171-178.
- Hong, S. D., Kim, Y. S., Kim, J. H. and Choi, S. M. (2002), "Simple tension testing for CFT column-to-beam

- connections at tension side with new diaphragm”, *Proc. of Int. Symp. on Steel Structure : The Second, Korean Society of Steel Structure*, 405-416.
- Kato, B. (1992), “Connection of beam flange to concrete-filled tubular column”, In: *Composite Construction in Steel and Concrete II - Proc. of an Engineering Foundation Conf.*, Missouri: 528-558.
- Mohammad, S. (1997), “State of the art of concrete-filled steel tubular columns”, *ACI Struct. J.* **94**, 558-571.
- SAC Joint Venture (2000a), “Recommended seismic design criteria for new steel moment frame buildings”, Rep. No. FEMA-350, Federal Emergency Management Agency, Washington, D.C.
- Schneider, S. P. and Alostaz, Y. M. (1998), “Experimental behavior of connections to concrete-filled steel tubes”, *J. Construct. Steel Res.*, **45**(3), 321-352.
- Storozhenko, L. Butsky, V. and Taranovsky, O. (1998), “Stability of compressed steel concrete composite tubular columns with centrifuged cores”, *J. Construct. Steel Res.*, **46**(1-3), pp. 484.
- Wang, Y. C. (1997), “Some considerations in the design of unprotected concrete-filled steel tubular columns under fire conditions”, *J. Construct. Steel Res.*, **44**, 203-223.
- Yun, Y. S., Kim, Y. S., Kim, J. H. and Choi, S. M. (2002), “Cyclic testing for CFT column-to-beam connections with new diaphragm”, *Proc. of Int. Symp. on Steel Structures: The Second, Korean Society of Steel Structures*, 440-451.
- Yun, Y. S., Kim, Y. S., Kim, J. H. and Choi, S. M. (2005), “A study on seismic performance for CFT square column-to-beam connections reinforced with asymmetric lower diaphragms”, *Proc. of Int. Symp. on Steel Structures : The Third, Korean Society of Steel Structures*, 409-421.